

Thalamotemporal impairment in temporal lobe epilepsy: A combined MRI analysis of structure, integrity, and connectivity

*†Simon S. Keller, ‡Jonathan O’Muircheartaigh, *Catherine Traynor, *Karren Towgood, ‡Gareth J. Barker, and *Mark P. Richardson

Epilepsia, 55(2):306–315, 2014

doi: 10.1111/epi.12520

SUMMARY

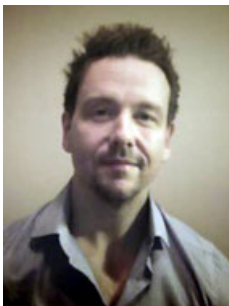
Objective: Thalamic abnormality in temporal lobe epilepsy (TLE) is well known from imaging studies, but evidence is lacking regarding connectivity profiles of the thalamus and their involvement in the disease process. We used a novel multisequence magnetic resonance imaging (MRI) protocol to elucidate the relationship between mesial temporal and thalamic pathology in TLE.

Methods: For 23 patients with TLE and 23 healthy controls, we performed T₁-weighted (for analysis of tissue structure), diffusion tensor imaging (tissue connectivity), and T₁ and T₂ relaxation (tissue integrity) MRI across the whole brain. We used connectivity-based segmentation to determine connectivity patterns of thalamus to ipsilateral cortical regions (occipital, parietal, prefrontal, postcentral, precentral, and temporal). We subsequently determined volumes, mean tractography streamlines, and mean T₁ and T₂ relaxometry values for each thalamic segment preferentially connecting to a given cortical region, and of the hippocampus and entorhinal cortex.

Results: As expected, patients had significant volume reduction and increased T₂ relaxation time in ipsilateral hippocampus and entorhinal cortex. There was bilateral volume loss, mean streamline reduction, and T₂ increase of the thalamic segment preferentially connected to temporal lobe, corresponding to anterior, dorsomedial, and pulvinar thalamic regions, with no evidence of significant change in any other thalamic segments. Left and right thalamotemporal segment volume and T₂ were significantly correlated with volume and T₂ of ipsilateral (epileptogenic), but not contralateral (nonepileptogenic), mesial temporal structures.

Significance: These convergent and robust data indicate that thalamic abnormality in TLE is restricted to the area of the thalamus that is preferentially connected to the epileptogenic temporal lobe. The degree of thalamic pathology is related to the extent of mesial temporal lobe damage in TLE.

KEY WORDS: Connectivity, Brain networks, Diffusion tensor imaging, Mesial temporal lobe, Thalamus.



Dr. Simon Keller is a lecturer and senior research scientist using advanced neuroimaging techniques in people with epilepsy.

Accepted November 22, 2013; Early View publication January 21, 2014.

*The Department of Clinical Neuroscience, Institute of Psychiatry, King’s College London, London, United Kingdom; †The Department of Molecular and Clinical Pharmacology, Institute of Translational Medicine, University of Liverpool, Liverpool, United Kingdom; and ‡The Department of Neuroimaging, Institute of Psychiatry, King’s College London, London, United Kingdom

Address correspondence to Simon S. Keller, Room 2:20, Clinical Sciences Centre, Aintree University Hospital and The Walton Centre NHS Foundation Trusts, Lower Lane, Liverpool L9 7LJ, U.K. E-mail: simon.keller@liverpool.ac.uk

© 2014 The Authors. *Epilepsia* published by Wiley Periodicals, Inc. on behalf of International League Against Epilepsy.

This is an open access article under the terms of the Creative Commons Attribution License, which permits use, distribution and reproduction in any medium, provided the original work is properly cited.

The thalamus modulates seizure activity and influences the propagation of seizures regardless of the location of the epileptogenic focus.¹ Thalamic stimulation for the relief of intractable seizures may significantly reduce seizure frequency in patients who have not responded optimally to antiepileptic drug and/or surgical treatment.^{2,3} However, the mechanisms underlying reduced seizure severity after thalamic stimulation are largely unknown. Comparative animal studies of limbic epilepsy have shown that medial thalamic nuclei are important for seizure modulation and spread⁴ and show consistent neuropathologic alteration,⁵ and that dorsomedial regions have an excitatory influence on the hippocampus.^{6,7} Furthermore, human electrophysiologic studies, in a very small number of patients, have shown that the posterior pulvinar regions of the thalamus show ictal changes in some patients with mesial temporal seizure onset.^{8,9} Anterior, dorsomedial, and pulvinar regions of the thalamus preferentially connect with the temporal lobe.¹⁰ A localized thalamotemporal network may therefore be affected in temporal lobe epilepsy (TLE). However, evidence is lacking regarding connectivity profiles of the thalamus and their involvement in the TLE disease process. Comprehensive reviews of magnetic resonance imaging (MRI) findings in TLE have reported that the thalamus is the most affected extrahippocampal brain region in patients with TLE.^{11,12} One study investigated the relationship between shape changes of the thalamus and multilobar neocortical thinning in patients with TLE.¹³ Another study reported volume alterations of the thalamus, which was correlated with cortical thinning of the temporal lobe.¹⁴ However, all aforementioned MRI studies have solely used MRI sequences from which little information on thalamocortical connectivity can be derived (e.g., T₁-weighted volume scans). Given (1) the opportunities to examine thalamocortical connectivity and integrity afforded by combining conventional MRI sequences with diffusion tensor imaging (DTI) and whole-brain relaxometry, and (2) the growing understanding of how network disruption may underlie seizure onset in focal and generalized epilepsies,^{15,16} it is increasingly important to examine the precise nature of thalamic involvement in TLE, and how thalamic alterations relate to temporal lobe abnormalities. In the present study, we recruited a sample of patients with TLE and healthy controls who each underwent an identical multisequence research MRI protocol with a primary objective of mapping alterations of thalamocortical connectivity and intrathalamic integrity in TLE, and their relationship with the disease process.

METHODS

Participants

We recruited 23 patients with well-characterized unilateral mesial TLE (11 left-onset; mean age 40.9 years) attending King's College Hospital London and 23 healthy controls (mean age 35.3 years; no significant difference

between patients and controls: $p = 0.37$). Diagnosis and localization of TLE was determined by comprehensive evaluation including detailed history and seizure semiology, scalp electroencephalography (EEG), intracranial EEG with video telemetry where necessary, and clinical MRI (T₁-weighted, T₂-weighted, and fluid-attenuated inversion recovery [FLAIR] scans). All patients had a history of complex partial seizures. In two cases, complex partial seizures were rare, and recurrent simple partial seizures were the primary seizure type. No patient had evidence of lesions other than unilateral hippocampal sclerosis diagnosed by an expert neuroradiologist. All patients had quantitative MRI evidence of unilateral hippocampal pathology ipsilateral to the side of the seizure focus determined by (1) volume loss on T₁-weighted images, (2) increased hippocampal T₂ values,¹⁷ or (3) a combination of both. Values were considered abnormal in patients if they were two standard deviations below (volume) or above (T₂) the mean of controls. Calculation of whole hippocampal volume and mean hippocampal T₂ values is described in the Supporting Information. Table 1 provides a summary of demographic and clinical data of patients and controls. The London-Dulwich Research Ethics Committee (formerly the King's College Hospital Research Ethics Committee) approved the study, and written informed consent was obtained from all participants.

MRI acquisition

All patients and controls were scanned using an identical MR protocol on a 3 Tesla GE Signa HDx system (General Electric, Waukesha, WI, U.S.A.), with actively shielded magnetic field gradients (maximum amplitude 40 mT/m). The protocol consisted of routinely prescribed localizers, routine diagnostic sequences (two dimensional [2D] FLAIR and T₂-weighted sequences), a three-dimensional (3D) T₁-weighted structural volume (Inversion Recovery Spoiled Gradient Recalled echo [IR-SPGR]), a DTI sequence,¹⁸ and a series of 3D sequences optimized for T₁ and T₂ mapping (Driven Equilibrium Single Pulse Observation of T₁ / T₂ [DESPOT]).^{19,20} Details on acquisition parameters are provided in the Supporting Information.

MRI analysis

We used connectivity-based segmentation (CBS) of the thalamus based on the original work of Behrens et al.¹⁰ to determine thalamocortical connectivity for each participant. Details of image analysis are provided in the Supporting Information. An overview of CBS of the thalamus is presented in Figure 1. Briefly, Freesurfer software (www.Freesurfer.net, version 5.1.0) was used to obtain thalamic seeds and lobar cortical targets (occipital, parietal, prefrontal, postcentral, precentral, and temporal) for CBS analyses, and hippocampal and entorhinal regions-of-interest from each participant's IR-SPGR image. CBS of the thalamus was performed using FMRIB's (The Oxford Centre for Functional Magnetic Resonance Imaging of the Brain)

Table 1. Demographic and clinical data						
Group	Females/males	Age	Age of onset of TLE	Duration of TLE	Seizure frequency	SGTCS
Controls	11/12	36.3 (8.1)	–	–	–	–
Left TLE	6/5	41.5 (8.3)	18.5 (14.3)	22.0 (17.2)	9.8 (10.7)	6
Right TLE	7/5	39.0 (11.7)	16.9 (13.2)	21.7 (12.3)	8.2 (8.4)	4

Data are mean (standard deviation, SD). Age, age of onset of TLE, and duration of TLE are recorded in years. Seizure frequency is number of seizures per month. SGTCS is number of patients experiencing secondary generalized tonic-clonic seizures.

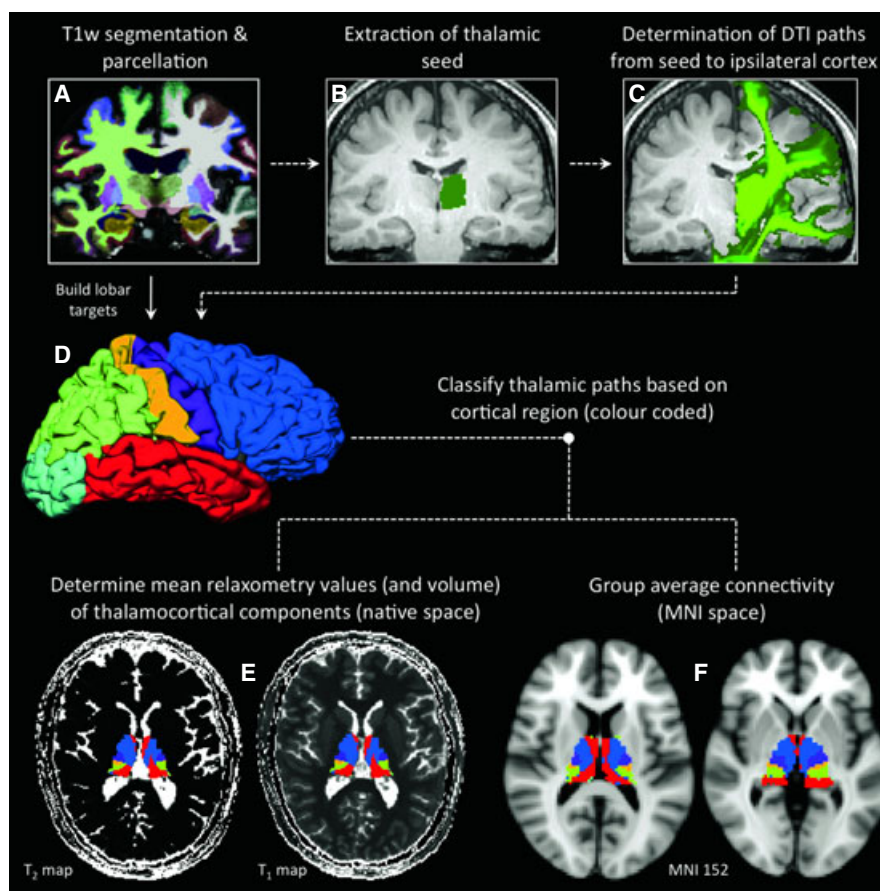


Figure 1.

Combining T_1 -weighted, DTI, and relaxometry data to determine thalamocortical connectivity using CBS. Subcortical segmentation, gray-white matter differentiation, and regional cortical (gyral) parcellation is performed on IR-SPGR (T_1 -weighted) data using Freesurfer (A), from which thalamic seeds are extracted (B) and lobar targets are built (D). After nonlinear registration between IR-SPGR and DTI data, connectivity paths are determined from the thalamic seed to ipsilateral hemispheric regions using FSL probtrackX (C). Thalamic paths are classified according to the cortical lobar target with which they preferentially connect using “find_the_biggest” function in FSL (E; red, temporal cortex; blue, prefrontal cortex; purple, precentral cortex; yellow, postcentral cortex; green, parietal cortex; turquoise, occipital cortex). After intrasubject registration between DTI data and relaxometry maps using FMRIB’s Linear Image Registration Tool (FLIRT), mean T_1 and T_2 values (and volumes) are calculated from each thalamocortical component (E). For group-wise average of thalamocortical segments (F), intersubject registration is applied using FMRIB’s Nonlinear Image Registration Tool (FNIRT) so that data is in standard space (Montreal Neurological Institute (MNI) space; see Supporting Information).

Epilepsia © ILAE

Diffusion Toolbox (FDT) for probabilistic tractography running in FSL (FMRIB Software Library, <http://fsl.fmrib.ox.ac.uk/fsl/fslwiki>) based on DTI and IR-SPGR data. The volume of each thalamic segment preferentially connecting with a cortical target region (e.g., thalamotemporal segment, thalamoparietal segment, etc.), and of the

hippocampus and entorhinal cortex, was calculated. Thalamocortical segment, hippocampal, and entorhinal volumes were analyzed, both corrected and uncorrected, for total intracranial volume (ICV); ICV was automatically obtained from Freesurfer segmentations. In order to visualize the topology of thalamocortical connectivity across

individuals, thalamocortical segments were nonlinearly spatially normalized to Montreal Neurological Institute (MNI) space and averaged (see Supporting Information).

We additionally determined three further MRI measures for each structure. Mean T_1 and T_2 relaxation values for each thalamocortical segment, hippocampus, and entorhinal cortex was obtained by coregistering the T_1 and T_2 maps determined using DESPOT acquisitions with the DTI and IR-SPGR images. Furthermore, we recorded the number of streamlines between thalamus and lobar target as a proportion of the number going to all target areas. As in previous studies,^{21,22} the mean value for all nonzero voxels in the seed area was calculated, and was corrected for total number of streamlines to all target regions, which provided the mean proportion of streamlines to each target area. The mean proportion of streamlines provides inferential information on the degree of connectivity between thalamus and lobar target.

Statistical analyses

Analyses were performed using SPSS (IBM Corp. Released 2012. IBM SPSS Statistics, Version 21.0.; Armonk, NY, U.S.A.). Volumetric, streamline, and relaxometry data for mesial temporal and thalamocortical segments were analyzed in each subject's native space using a multivariate analysis of variance (ANOVA) including group (control, left TLE, right TLE) as a fixed factor, and brain structure volume, mean number of streamlines, and mean T_1 and T_2 as dependent variables. Given the large number of comparisons ($6 \times$ thalamocortical segments, $2 \times$ mesial temporal lobe structures, $4 \times$ MRI measures [volume, streamlines, T_1 and T_2], $2 \times$ hemispheres, $3 \times$ groups), post hoc Bonferroni corrections were performed to resolve the direction of main effects and correct for multiple comparisons. Although there was no significant difference in mean age between patients and controls, we included age as a nuisance factor in analyses given the slightly older age of patients. Pearson's correlations were used to examine relationships between volume, mean streamlines, mean T_1 and T_2 values, and clinical variables. We restricted correlations between brain regions to values from the same MRI sequence (i.e., volume with volume, T_1 with T_1 , and T_2 with T_2). Given that mean streamlines are obtained only for each thalamocortical segment, streamlines were only correlated with clinical variables and not mesial temporal values from other sequences.

RESULTS

All main effects and F-values are tabulated in the Supporting Information.

Medial temporal lobe

There were significant main effects of left entorhinal volume ($F = 11.09$, $p < 0.001$) and T_2 ($F = 9.15$, $p = 0.001$),

right entorhinal volume ($F = 6.05$, $p = 0.005$) and T_2 ($F = 8.51$, $p = 0.001$), left hippocampal volume ($F = 9.43$, $p < 0.001$), T_1 ($F = 4.90$, $p = 0.01$), and T_2 ($F = 7.39$, $p = 0.002$), and right hippocampal volume ($F = 10.12$, $p < 0.001$) and T_2 ($F = 3.49$, $p = 0.04$). Post hoc Bonferroni corrected results (Table 2) indicated decreased volume of the ipsilateral entorhinal cortex (left TLE: $p < 0.001$; right TLE: $p = 0.005$) and hippocampus (left TLE: $p < 0.001$; right TLE: $p < 0.001$) in patients relative to controls. These findings were also obtained when corrected for ICV. Mean T_2 values were significantly increased in the ipsilateral entorhinal cortex (left TLE: $p < 0.001$; right TLE: $p < 0.001$) and hippocampus (left TLE: $p = 0.002$; right TLE: $p = 0.045$) in patients relative to controls. There was also a significant increase in mean T_2 of the contralateral entorhinal cortex in patients with left TLE relative to controls ($p = 0.02$).

Connectivity-based thalamic segmentation

There were significant main effects of the volume of the left thalamoparietal segment ($F = 4.03$, $p = 0.03$), thalamopostcentral segment ($F = 3.51$, $p = 0.04$), thalamotemporal segment ($F = 21.52$, $p < 0.001$), whole thalamus ($F = 6.53$, $p = 0.003$), and right thalamotemporal segment ($F = 17.96$, $p < 0.001$). The remaining significant main

Table 2. Post hoc Bonferroni-corrected differences in mesial temporal lobe regions between patients and controls.

Region	Hemisphere	Measure	Comparison	Bonferroni Sig.
Entorhinal	L	Volume	Ctrl-L TLE	0.000***
			Ctrl-R TLE	0.033*
		T_1	Ctrl-L TLE	0.147
			Ctrl-R TLE	1.00
		T_2	Ctrl-L TLE	0.000***
			Ctrl-R TLE	0.560
	R	Volume	Ctrl-L TLE	1.00
			Ctrl-R TLE	0.005***
		T_1	Ctrl-L TLE	0.374
			Ctrl-R TLE	1.00
		T_2	Ctrl-L TLE	0.020*
			Ctrl-R TLE	0.000***
Hippocampus	L	Volume	Ctrl-L TLE	0.000***
			Ctrl-R TLE	1.00
		T_1	Ctrl-L TLE	0.035*
			Ctrl-R TLE	1.00
		T_2	Ctrl-L TLE	0.002***
			Ctrl-R TLE	1.00
	R	Volume	Ctrl-L TLE	1.00
			Ctrl-R TLE	0.000***
		T_1	Ctrl-L TLE	0.542
			Ctrl-R TLE	0.214
		T_2	Ctrl-L TLE	0.409
			Ctrl-R TLE	0.045*

*** $p < 0.001$; ** $p < 0.01$; * $p < 0.05$.

Main effects and corresponding F values are provided in the Supporting Information

effects were restricted to left and right thalamotemporal mean T_2 ($F = 14.99$, $p < 0.001$ and $F = 5.53$, $p = 0.007$, respectively) and left and right thalamotemporal mean number of streamlines ($F = 5.27$, $p = 0.009$ and $F = 7.43$, $p = 0.002$, respectively). Table 3 presents the Bonferroni corrected results, and indicates that other than significantly reduced ipsilateral whole thalamic volume in patients with left TLE relative to controls ($p = 0.002$), all significant differences in volume, mean T_2 and mean number of streamlines between patients and controls were restricted to the left and right thalamotemporal segments. This included reduction in ipsilateral (left TLE $p < 0.001$, right TLE $p < 0.001$) and contralateral (left TLE $p = 0.001$, right TLE $p < 0.001$) volume, increased ipsilateral (left TLE $p < 0.001$, right TLE $p = 0.04$) and contralateral (left TLE $p = 0.02$, right TLE $p < 0.001$) mean T_2 , and reduced ipsilateral (left TLE $p = 0.03$, right TLE $p = 0.04$) and contralateral (left TLE only $p = 0.001$) mean number of streamlines, in patients relative to controls. These combined thalamotemporal alterations are illustrated in Figure 2. Although not achieving statistical significance, there were nonspecific increases in the corrected number of streamlines and volume of other thalamocortical segments in patients relative to controls. In particular, there was a strong trend for an increased number of streamlines within the thalamoprecentral segment in patients relative to controls ($p = 0.07$, Table 3). Significant reduction of thalamotemporal segment volume in patients was also seen when corrected for ICV and whole thalamic volume. The spatial organization of the averaged thalamocortical segments across individuals can be visualized in Figure 1F and in more detail in the Supporting Information. In particular, the thalamotemporal segment that showed the only differences in structure, integrity, and connectivity in patients was located in anterior, dorso-medial, and posterior thalamic regions.

Correlations and clinical variables

Given that significant differences between patients and controls were limited to mesial temporal structures and thalamotemporal segments, we restricted correlation analyses to these regions. Furthermore, because patients with left and right TLE showed similar mesial temporal and thalamotemporal segment alterations, we combined patients with left- and right-sided TLE into one sample for correlational analyses to increase statistical sensitivity, and treated structures as ipsilateral and contralateral to the epileptogenic focus. Correlational analyses indicated that ipsilateral hippocampal and entorhinal volume were significantly correlated with ipsilateral ($r = 0.39$, $p = 0.008$ and $r = 0.58$, $p < 0.001$, respectively) and contralateral ($r = 0.39$, $p = 0.02$ and $r = 0.52$, $p < 0.001$, respectively) thalamotemporal segment volume. Similarly, ipsilateral hippocampal and entorhinal mean T_2 values were correlated with ipsilateral ($r = 0.45$, $p = 0.002$ and $r = 0.55$,

Table 3. Post hoc Bonferroni-corrected differences in thalamocortical segments between patients and controls.

Region	Hemisphere	Measure	Comparison	Bonferroni Sig.
Thalamus: occipital	L	Volume	Ctrl–L TLE	0.471
			Ctrl–R TLE	1.00
		T_1	Ctrl–L TLE	1.00
			Ctrl–R TLE	1.00
		T_2	Ctrl–L TLE	1.00
			Ctrl–R TLE	1.00
	Streamlines	Ctrl–L TLE	0.355	
		Ctrl–R TLE	1.00	
	R	Volume	Ctrl–L TLE	1.00
			Ctrl–R TLE	0.872
		T_1	Ctrl–L TLE	0.079
			Ctrl–R TLE	0.533
T_2		Ctrl–L TLE	1.00	
		Ctrl–R TLE	1.00	
Streamlines	Ctrl–L TLE	0.447		
	Ctrl–R TLE	1.00		
Thalamus: parietal	L	Volume	Ctrl–L TLE	0.058
			Ctrl–R TLE	0.337
		T_1	Ctrl–L TLE	1.00
			Ctrl–R TLE	1.00
		T_2	Ctrl–L TLE	1.00
			Ctrl–R TLE	1.00
	Streamlines	Ctrl–L TLE	0.534	
		Ctrl–R TLE	1.00	
	R	Volume	Ctrl–L TLE	0.708
			Ctrl–R TLE	0.332
		T_1	Ctrl–L TLE	1.00
			Ctrl–R TLE	0.690
T_2		Ctrl–L TLE	1.00	
		Ctrl–R TLE	1.00	
Streamlines	Ctrl–L TLE	1.00		
	Ctrl–R TLE	1.00		
Thalamus: PFC	L	Volume	Ctrl–L TLE	1.00
			Ctrl–R TLE	1.00
		T_1	Ctrl–L TLE	1.00
			Ctrl–R TLE	1.00
		T_2	Ctrl–L TLE	1.00
			Ctrl–R TLE	1.00
	Streamlines	Ctrl–L TLE	1.00	
		Ctrl–R TLE	1.00	
	R	Volume	Ctrl–L TLE	1.00
			Ctrl–R TLE	1.00
		T_1	Ctrl–L TLE	1.00
			Ctrl–R TLE	5.13
T_2		Ctrl–L TLE	1.00	
		Ctrl–R TLE	1.00	
Streamlines	Ctrl–L TLE	0.45		
	Ctrl–R TLE	0.98		
Thalamus: postcentral	L	Volume	Ctrl–L TLE	0.124
			Ctrl–R TLE	0.100
		T_1	Ctrl–L TLE	1.00
			Ctrl–R TLE	1.00
		T_2	Ctrl–L TLE	1.00
			Ctrl–R TLE	1.00
	Streamlines	Ctrl–L TLE	1.00	
		Ctrl–R TLE	1.00	
	R	Volume	Ctrl–L TLE	1.00
			Ctrl–R TLE	1.00

Continued

Table 3. Continued.

Region	Hemisphere	Measure	Comparison	Bonferroni Sig.
Thalamus: precentral	L	T ₁	Ctrl-L TLE	0.487
			Ctrl-R TLE	1.00
		T ₂	Ctrl-L TLE	1.00
			Ctrl-R TLE	0.722
		Streamlines	Ctrl-L TLE	0.42
			Ctrl-R TLE	0.65
		Volume	Ctrl-L TLE	1.00
	Ctrl-R TLE		1.00	
	R	T ₁	Ctrl-L TLE	0.985
			Ctrl-R TLE	1.00
		T ₂	Ctrl-L TLE	1.00
			Ctrl-R TLE	0.834
		Streamlines	Ctrl-L TLE	1.00
			Ctrl-R TLE	1.00
Volume		Ctrl-L TLE	1.00	
	Ctrl-R TLE	0.692		
Thalamus: temporal	L	T ₁	Ctrl-L TLE	1.00
			Ctrl-R TLE	1.00
		T ₂	Ctrl-L TLE	0.000***
			Ctrl-R TLE	0.000***
		Streamlines	Ctrl-L TLE	0.034*
			Ctrl-R TLE	0.304
		Volume	Ctrl-L TLE	0.001**
	Ctrl-R TLE		0.000***	
	R	T ₁	Ctrl-L TLE	1.00
			Ctrl-R TLE	0.227
		T ₂	Ctrl-L TLE	0.024*
			Ctrl-R TLE	0.038*
		Streamlines	Ctrl-L TLE	0.001**
			Ctrl-R TLE	0.041*
Volume		Ctrl-L TLE	0.002**	
	Ctrl-R TLE	0.114		
Thalamus: whole	L	T ₁	Ctrl-L TLE	0.772
			Ctrl-R TLE	1.00
		T ₂	Ctrl-L TLE	0.243
			Ctrl-R TLE	1.00
		Streamlines	Ctrl-L TLE	–
			Ctrl-R TLE	–
		Volume	Ctrl-L TLE	0.173
	Ctrl-R TLE		0.231	
	R	T ₁	Ctrl-L TLE	1.00
			Ctrl-R TLE	0.174
		T ₂	Ctrl-L TLE	1.00
			Ctrl-R TLE	0.413
		Streamlines	Ctrl-L TLE	–
			Ctrl-R TLE	–

***p < 0.001; **p < 0.01; *p < 0.05.

Main effects and corresponding F values are provided in the Supporting Information. Statistically significant differences between patients and controls are restricted to thalamotemporal segment volume, T₂ and streamlines, with no significant effects in any other segment. Ipsilateral whole thalamic volume is also significantly reduced in patients with left TLE. Analysis of thalamocortical segment streamlines are performed corrected for total number of streamlines

p < 0.001, respectively) and contralateral (r = 0.63, p < 0.001 and r = 0.35, p < 0.02, respectively) thalamo-temporal segment mean T₂. Ipsilateral mesial temporal and thalamotemporal correlations are shown in Figure 3. There were no correlations with contralateral (i.e., nonepileptogenic) mesial temporal structures. Ipsilateral thalamocortical segment mean T₂ was correlated with duration of epilepsy (number of years; r = 0.48, p = 0.02) and seizure frequency (number of complex partial seizures per year; r = 0.45, p = 0.03). Ipsilateral thalamocortical segment mean number of streamlines was also correlated with seizure frequency (r = -0.44, p = 0.03). There were no other statistically significant relationships.

DISCUSSION

The thalamus is known to be a crucial component of the seizure-generating network in generalized spike-wave, which is characteristic of idiopathic (or genetic) generalized epilepsy (IGE).²³ Global structural impairments (e.g., volume loss) of the thalamus have been reported previously in IGE.^{24,25} Prior evidence strongly suggests that thalamus is affected in epilepsies with focal-onset seizures, possibly as part of a seizure-generating network,²⁶ although specific details of the involvement of thalamus in human TLE are lacking. In TLE, thalamic involvement has typically been reported in terms of nonspecific global volume loss,^{1,12,14} or nonspecific DTI-determined diffusion abnormalities.^{27,28} However, the thalamus has a complex internal structure, sending and receiving connections to different cortical regions across the entire brain from different regions within the thalamus. In the present study we report for the first time that the specific regions of the thalamus that were demonstrated to preferentially connect with the temporal lobe are abnormal bilaterally in TLE, and that the severity of abnormality is correlated with the degree of mesial temporal damage in the epileptogenic temporal lobe. Regions of the thalamus that were demonstrated to be preferentially connected with other brain regions showed no pathologic change.

The organization of thalamocortical connections in this paper is consistent with the work of Behrens et al.¹⁰ in healthy controls, indicating that the temporal lobe preferentially connects with anterior, dorsomedial, and posterior regions of the thalamus (see Fig. 1F and Supporting Information), corresponding to the anterior nuclear group, the dorsomedial nucleus, and the pulvinar, respectively. It is these thalamic nuclear regions that are abnormal in terms of structure, connectivity (as suggested in analysis of volume and DTI streamlines) and integrity (T₂ relaxometry) in patients with TLE. Our data are consistent with, build on, and integrate previous studies that report:

1. that dorsomedial thalamic regions have an excitatory influence on the hippocampus in animal models;^{6,7}

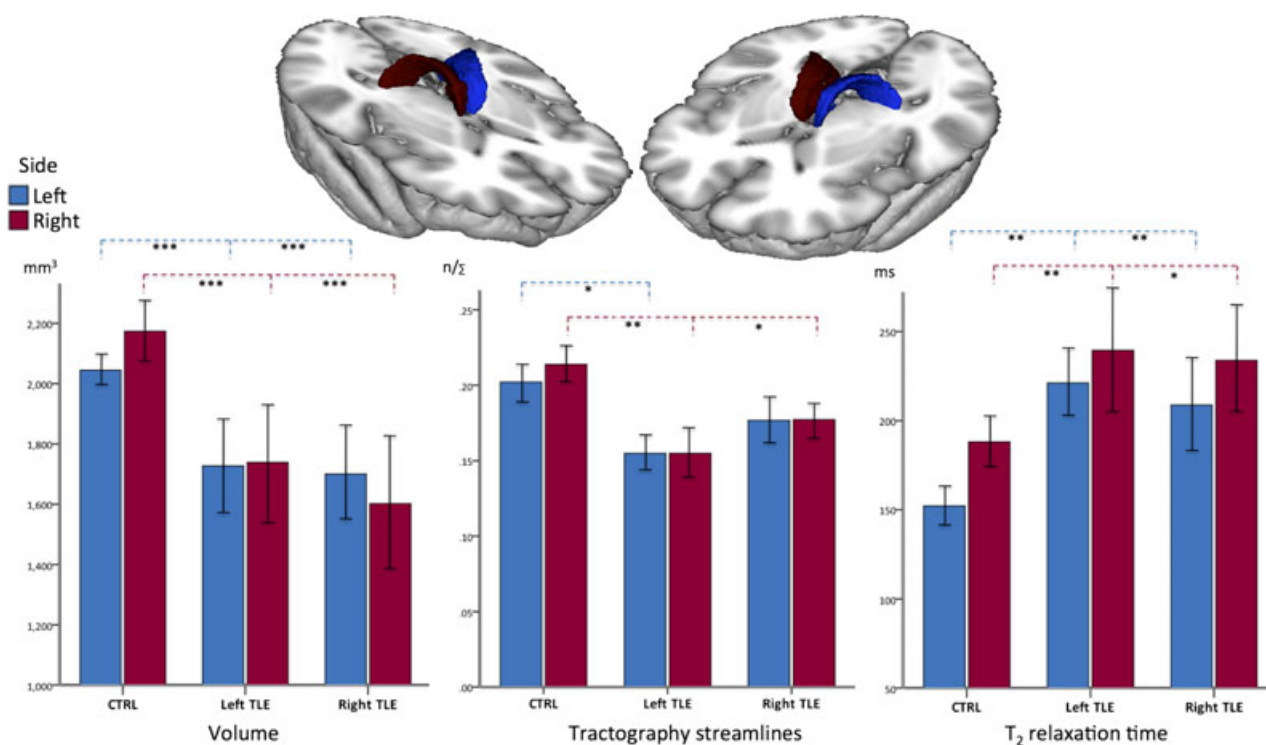


Figure 2.

Differences in volume, proportional number of tractography streamlines, and T_2 relaxation of the ipsilateral and contralateral thalamo-temporal segments in patients relative to controls. Top: Three-dimensional rendering of the left (blue) and right (red) thalamo-temporal segments averaged from all subjects in MNI space (see Supporting Information). Bottom left: volume reduction in patients relative to controls. Bottom middle: corrected mean number of tractography streamlines reduced in patients relative to controls. Bottom right: T_2 relaxation increase in patients relative to controls. Blue and red bars represent the left and right thalamo-temporal segments, respectively. *** $p < 0.001$; ** $p < 0.01$; * $p < 0.05$.

Epilepsia © ILAE

- neuronal loss and physiologic alterations in the dorsomedial thalamus in animal models of limbic epilepsy;^{4,5}
- shape alterations of the thalamus in regions hypothesized—but not demonstrated—to be connected to the temporal lobe in TLE;¹³
- preferential gray matter loss of a region corresponding to the dorsomedial area of the thalamus in a recent review of voxel-based morphometry studies of TLE;¹¹
- 2-deoxy-2-[¹⁸F]fluoro-D-glucose and [¹¹C]flumazenil positron emission tomography (PET) abnormalities of the dorsomedial thalamic region in patients with TLE;²⁹
- ictal changes in the pulvinar during mesial temporal lobe seizures based on stereoelectroencephalographic (SEEG) data in a small number of cases.^{8,9}

Despite the fact that structural and metabolic alterations of the medial temporal lobe^{12,30} and thalamus^{1,12,30} are frequently reported in TLE, there are few studies examining altered connectivity between the temporal lobe and thalamus in these patients, which would provide more direct evidence of an epileptogenic network. Correlating neural dysfunction³⁰ and measures of atrophy^{13,14} between thalamus and temporal lobe has been suggestive of thalamo-temporal network pathology, but there have been no

attempts to identify regional thalamic alterations based on the determined cortical connectivity patterns of the thalamus, using multiple measures of tissue alteration. Mueller et al.¹⁴ and Bonilha et al.³¹ provided evidence of region-specific atrophy of the anterior thalamus in TLE, while Bernhardt et al.¹³ reported atrophy of anterior, medial, and posterior thalamus. Despite that the aforementioned authors describe alterations of the thalamus in context of its connectivity with the temporal lobe, all evidence of thalamic structural alteration was derived from T_1 -weighted MRI scans only, which provides very little—if any—information on brain connectivity. Our data are more consistent with that of Bernhardt et al.¹³ in terms of the spatial topology of thalamic abnormality, but we delineate the thalamic region preferentially connecting to the temporal lobe, and provide combined measures of region-specific thalamic pathology based on a multisequence MRI approach.

The etiology of thalamo-temporal abnormalities in TLE is difficult to resolve. Competing hypotheses of excitotoxic damage and deafferentation have been proposed to explain extrahippocampal atrophy in TLE, and it is possible that both mechanisms play a role in thalamic damage. Our finding of correlations between the extent of ipsilateral mesial

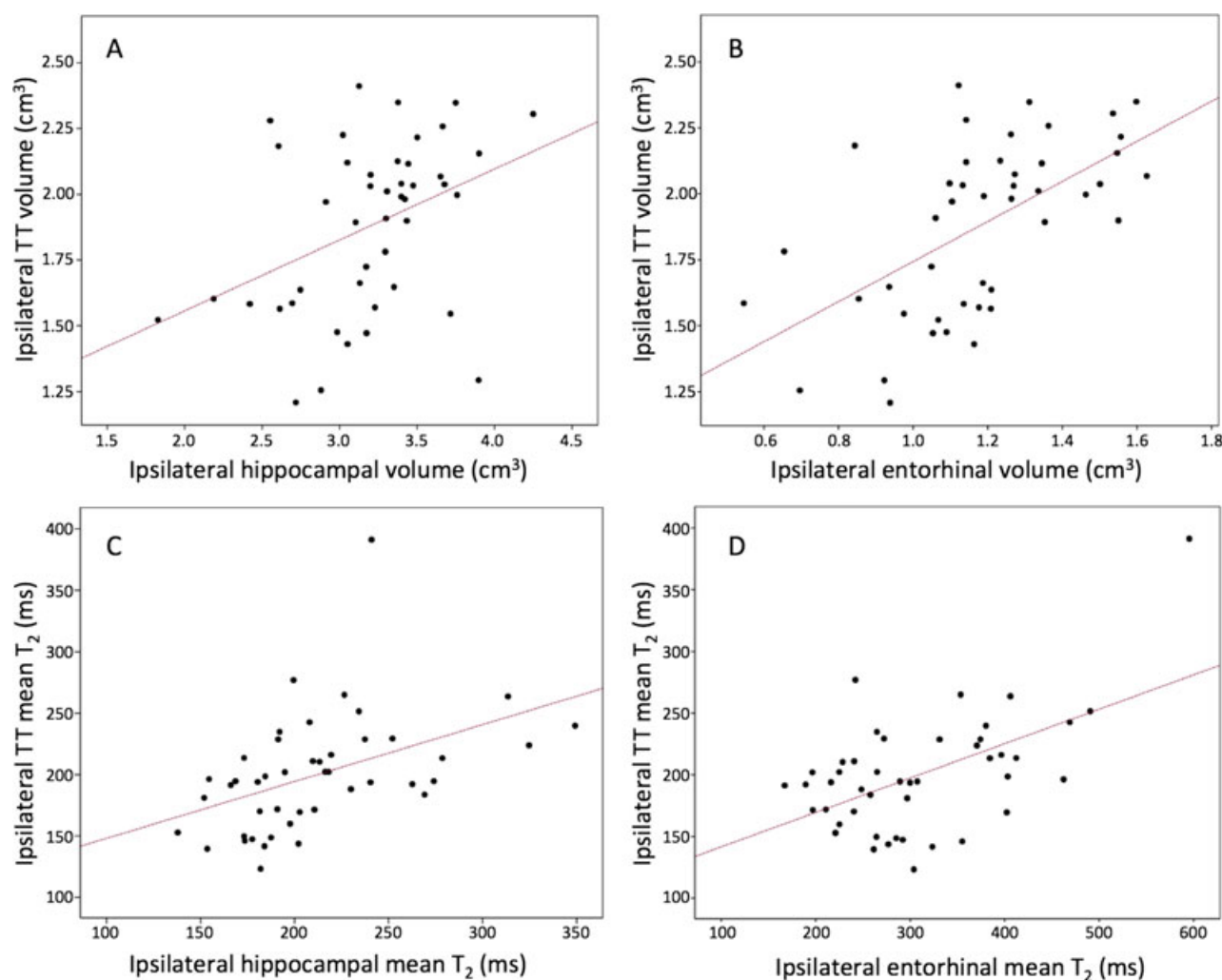


Figure 3.

Significant correlations between ipsilateral mesial temporal and thalamotemporal (TT) structures. **(A)** hippocampal and TT volume; **(B)** entorhinal and TT volume; **(C)** hippocampal and TT mean T_2 ; **(D)** entorhinal and TT mean T_2 . Correlations were also observed between the ipsilateral mesial temporal and contralateral TT structures (not pictured, see main text), but not with contralateral mesial temporal structures.

Epilepsia © ILAE

temporal and thalamotemporal segment damage are somewhat consistent with that of Mueller et al.,¹⁴ who reported a relationship between volume loss of the thalamus and cortical thinning of the mesial temporal lobe, and interpreted these results as suggestive of progressive thalamic degeneration due to seizure propagation from the connected epileptogenic temporal lobe. Barron et al.¹¹ also suggested that thalamic damage could result from mesial temporal excitotoxicity, given that the epileptogenic hippocampus and dorsomedial area of the thalamus are nodes within the same network, thereby providing a route for excitotoxic damage. These interpretations are partially supported by our data that indicate that the degree of the thalamic damage is correlated with the extent of damage to the epileptogenic mesial temporal lobe but not the contralateral side. In conjunction with commissural and brainstem mediated spread, the thalamus

serves as an interhemispheric ictal propagation pathway,³² which may in part explain the bilateral thalamotemporal damage observed in this study. Furthermore, the extent of thalamic damage appears to be related to duration of epilepsy (as indicated in this study and in others^{27,33}), which may be suggestive of a degenerative effect on the thalamus due to the chronicity of TLE.³⁴

On the other hand, Bonilha et al.³⁵ suggested that the excitotoxic effects of seizures would be reduced when the epileptogenic zone becomes increasingly disconnected from other cortical and subcortical regions, and that such disconnection may also contribute to neuronal damage in some brain regions. Our results are also in support of this, given that a circumscribed loss of thalamotemporal segment volume and reduction of mean streamlines is suggestive of reduced structural connectiv-

ity between the temporal lobe and thalamus. Thalamo-temporal deafferentation is a plausible hypothesis in light of findings from a recent computer simulation study of EEG data that indicated that decreasing connectivity between brain regions increases the frequency of seizure-like activity.¹⁶ This seemingly counterintuitive finding may be explained by the notion of fewer connections creating a less stable network, which may facilitate the transition to ictal dynamics.¹⁵ There has been a recent move to understand how seizures begin and terminate through the study of macrostructural networks using animal models, neuroimaging data, and simulated data;¹⁶ loss of connectivity between brain regions is a legitimate hypothesis for the etiology of both focal and generalized seizures. This new direction of research mirrors recent modifications in the classification of epilepsy disorders to consider the importance of brain networks for seizure onset, even in focal epilepsies.^{36,37} Our findings of reduced thalamotemporal connectivity in patients with TLE are consistent with other data indicating loss of general temporal lobe connectivity,³⁸ and together suggest that the phenomenologic concept of network disruption causing seizures has an anatomic basis.

It is important to highlight pertinent methodologic issues. Firstly, we present data on a sample size smaller than many structural MRI studies of TLE, including work from some members of our research team.^{27,33,39} It is likely that the majority of previous structural MRI work in TLE has been performed in context of routine clinical/presurgical evaluation, and has benefited from routinely acquired MRIs. Here, we prospectively recruited patients and controls for a multisequence MRI research protocol specifically to investigate how the brain is altered in terms of structure, integrity, and connectivity in TLE, which is typically beyond the scope of clinical MRI protocols. Despite the relatively small sample size, we present very robust statistical evidence of circumscribed thalamotemporal pathology in TLE. Secondly, CBS and DTI are not without limitations. An in-depth critique of DTI is beyond the scope of this paper, and the reader is referred to an excellent recent discussion by Jones et al.⁴⁰ that covers a wide and detailed range of issues and considerations for all DTI research in clinical populations. Of particular relevance to the present study are the difficulties in modelling crossing fibers within a single voxel, the relatively low isotropic voxel size used, and the recommendations for increased number of gradient orientations. Furthermore, CBS only provides a relative value of thalamocortical segment connectivity; where we observed reduced connectivity streamlines in thalamotemporal segments in patients, there were nonspecific concomitant increases in other thalamocortical segments. Given that segments with fewer connectivity streamlines will always be accompanied by increased streamlines in other ipsilateral thalamic segments, such is the nature of the technique, it is wise to exercise caution

when interpreting intrathalamic reorganization using this method. However, our finding of selective involvement of the thalamotemporal segment is reinforced by the circumscribed increase in T_2 , the calculation of which is not dependent on the CBS technique.

CONCLUSION

Thalamic abnormality in TLE is restricted to the area of the thalamus that is preferentially connected with the epileptogenic temporal lobe. Although it is impossible to determine the directionality of any influences between brain regions using these neuroimaging data (i.e., do mesial temporal seizures cause damage to specific connected thalamic regions, does the disease process in specific thalamic regions permit increasingly degenerative changes of the epileptogenic temporal lobe, or are the two structures affected simultaneously), we do provide convincing evidence of a relationship between the degree of circumscribed thalamotemporal segment pathology and the extent of abnormality within the epileptogenic mesial temporal lobe.

ACKNOWLEDGMENTS

This work was supported by an Epilepsy Research UK Project Grant. JOM is supported by a Sir Henry Wellcome Postdoctoral Fellowship awarded by the Wellcome Trust (No 096195). We thank Dr. Andrew Simmons at the Department of Neuroimaging, Institute of Psychiatry, King's College London, for assistance with Freesurfer processing of SPGR images.

DISCLOSURE

Prof. Barker received honoraria from General Electric Healthcare, and from IXICO, at the time of this work. The remaining authors have no conflicts of interest. We confirm that we have read the Journal's position on issues involved in ethical publication and affirm that this report is consistent with those guidelines.

REFERENCES

1. Dreifuss S, Vingerhoets FJ, Lazeyras F, et al. Volumetric measurements of subcortical nuclei in patients with temporal lobe epilepsy. *Neurology* 2001;57:1636–1641.
2. Lim SN, Lee ST, Tsai YT, et al. Electrical stimulation of the anterior nucleus of the thalamus for intractable epilepsy: a long-term follow-up study. *Epilepsia* 2007;48:342–347.
3. Fisher R, Salanova V, Witt T, et al. Electrical stimulation of the anterior nucleus of thalamus for treatment of refractory epilepsy. *Epilepsia* 2010;51:899–908.
4. Bertram EH, Mangan PS, Zhang D, et al. The midline thalamus: alterations and a potential role in limbic epilepsy. *Epilepsia* 2001;42:967–978.
5. Bertram EH, Scott C. The pathological substrate of limbic epilepsy: neuronal loss in the medial dorsal thalamic nucleus as the consistent change. *Epilepsia* 2000;41(Suppl. 6):S3–S8.
6. Dolleman-Van der Weel MJ, Lopes da Silva FH, Witter MP. Nucleus reuniens thalami modulates activity in hippocampal field CA1 through excitatory and inhibitory mechanisms. *J Neurosci* 1997;17:5640–5650.
7. Bertram EH, Zhang DX. Thalamic excitation of hippocampal CA1 neurons: a comparison with the effects of CA3 stimulation. *Neuroscience* 1999;92:15–26.

8. Rosenberg DS, Mauguiere F, Demarquay G, et al. Involvement of medial pulvinar thalamic nucleus in human temporal lobe seizures. *Epilepsia* 2006;47:98–107.
9. Guye M, Regis J, Tamura M, et al. The role of corticothalamic coupling in human temporal lobe epilepsy. *Brain* 2006;129:1917–1928.
10. Behrens TE, Johansen-Berg H, Woolrich MW, et al. Non-invasive mapping of connections between human thalamus and cortex using diffusion imaging. *Nat Neurosci* 2003;6:750–757.
11. Barron DS, Fox PM, Laird AR, et al. Thalamic medial dorsal nucleus atrophy in medial temporal lobe epilepsy: a VBM meta-analysis. *Neuroimage Clin* 2013;2:25–32.
12. Keller SS, Roberts N. Voxel-based morphometry of temporal lobe epilepsy: an introduction and review of the literature. *Epilepsia* 2008;49:741–757.
13. Bernhardt BC, Bernasconi N, Kim H, et al. Mapping thalamocortical network pathology in temporal lobe epilepsy. *Neurology* 2012;78:129–136.
14. Mueller SG, Laxer KD, Barakos J, et al. Involvement of the thalamocortical network in TLE with and without mesiotemporal sclerosis. *Epilepsia* 2010;51:1436–1445.
15. Richardson MP. Large scale brain models of epilepsy: dynamics meets connectomics. *J Neurol Neurosurg Psychiatry* 2012;83:1238–1248.
16. Terry JR, Benjamin O, Richardson MP. Seizure generation: the role of nodes and networks. *Epilepsia* 2012;53:e166–e169.
17. Bernasconi A, Bernasconi N, Caramanos Z, et al. T2 relaxometry can lateralize mesial temporal lobe epilepsy in patients with normal MRI. *Neuroimage* 2000;12:739–746.
18. Jones DK, Williams SC, Gasston D, et al. Isotropic resolution diffusion tensor imaging with whole brain acquisition in a clinically acceptable time. *Hum Brain Mapp* 2002;15:216–230.
19. Deoni SC. High-resolution T1 mapping of the brain at 3T with driven equilibrium single pulse observation of T1 with high-speed incorporation of RF field inhomogeneities (DESPOT1-HIFI). *J Magn Reson Imaging* 2007;26:1106–1111.
20. Deoni SC. Transverse relaxation time (T2) mapping in the brain with off-resonance correction using phase-cycled steady-state free precession imaging. *J Magn Reson Imaging* 2009;30:411–417.
21. Rushworth MF, Behrens TE, Johansen-Berg H. Connection patterns distinguish 3 regions of human parietal cortex. *Cereb Cortex* 2006;16:1418–1430.
22. Croxson PL, Johansen-Berg H, Behrens TE, et al. Quantitative investigation of connections of the prefrontal cortex in the human and macaque using probabilistic diffusion tractography. *J Neurosci* 2005;25:8854–8866.
23. Blumenfeld H. Cellular and network mechanisms of spike-wave seizures. *Epilepsia* 2005;46(Suppl. 9):21–33.
24. Kim JH, Kim JB, Seo WK, et al. Volumetric and shape analysis of thalamus in idiopathic generalized epilepsy. *J Neurol* 2013;260:1846–1854.
25. Du H, Zhang Y, Xie B, et al. Regional atrophy of the basal ganglia and thalamus in idiopathic generalized epilepsy. *J Magn Reson Imaging* 2011;33:817–821.
26. Laufs H. Functional imaging of seizures and epilepsy: evolution from zones to networks. *Curr Opin Neurol* 2012;25:194–200.
27. Keller SS, Schoene-Bake JC, Gerdes JS, et al. Concomitant fractional anisotropy and volumetric abnormalities in temporal lobe epilepsy: cross-sectional evidence for progressive neurologic injury. *PLoS ONE* 2012;7:e46791.
28. Gong G, Concha L, Beaulieu C, et al. Thalamic diffusion and volumetry in temporal lobe epilepsy with and without mesial temporal sclerosis. *Epilepsy Res* 2008;80:184–193.
29. Juhasz C, Nagy F, Watson C, et al. Glucose and [11C]flumazenil positron emission tomography abnormalities of thalamic nuclei in temporal lobe epilepsy. *Neurology* 1999;53:2037–2045.
30. Hetherington HP, Kuzniecky RI, Vives K, et al. A subcortical network of dysfunction in TLE measured by magnetic resonance spectroscopy. *Neurology* 2007;69:2256–2265.
31. Bonilha L, Rorden C, Castellano G, et al. Voxel-based morphometry of the thalamus in patients with refractory medial temporal lobe epilepsy. *Neuroimage* 2005;25:1016–1021.
32. Blume WT. Clinical intracranial overview of seizure synchrony and spread. *Can J Neurol Sci* 2009;36(Suppl. 2):S55–S57.
33. Keller SS, Wieshmann UC, Mackay CE, et al. Voxel based morphometry of grey matter abnormalities in patients with medically intractable temporal lobe epilepsy: effects of side of seizure onset and epilepsy duration. *J Neurol Neurosurg Psychiatry* 2002a;73:648–655.
34. Benedek K, Juhasz C, Muzik O, et al. Metabolic changes of subcortical structures in intractable focal epilepsy. *Epilepsia* 2004;45:1100–1105.
35. Bonilha L, Edwards JC, Kinsman SL, et al. Extrahippocampal gray matter loss and hippocampal deafferentation in patients with temporal lobe epilepsy. *Epilepsia* 2010;51:519–528.
36. Berg AT, Berkovic SF, Brodie MJ, et al. Revised terminology and concepts for organization of seizures and epilepsies: report of the ILAE Commission on Classification and Terminology, 2005–2009. *Epilepsia* 2010;51:676–685.
37. Berg AT, Scheffer IE. New concepts in classification of the epilepsies: entering the 21st century. *Epilepsia* 2011;52:1058–1062.
38. Concha L, Kim H, Bernasconi A, et al. Spatial patterns of water diffusion along white matter tracts in temporal lobe epilepsy. *Neurology* 2012;79:455–462.
39. Keller SS, Mackay CE, Barrick TR, et al. Voxel-based morphometric comparison of hippocampal and extrahippocampal abnormalities in patients with left and right hippocampal atrophy. *Neuroimage* 2002b;16:23–31.
40. Jones DK, Knosche TR, Turner R. White matter integrity, fiber count, and other fallacies: the do's and don'ts of diffusion MRI. *Neuroimage* 2013;73:239–254.

SUPPORTING INFORMATION

Additional Supporting Information may be found in the online version of this article:

Data S1. Methods and results.